

EFFECT OF PARTICLE SIZE ON THE CHARACTERIZATION OF BINDERLESS PARTICLEBOARD MADE FROM *RHIZOPHORA spp.* MANGROVE WOOD FOR USE AS PHANTOM MATERIAL

Mohammad Wasef Marashdeh,^a Rokiah Hashim,^{b,*} Abd Aziz Tajuddin,^a Sabar Bauk,^c and Othman Sulaiman^b

Experimental binderless particleboards were made from various sizes of *Rhizophora spp.* particles. The experimental samples were made by cold pressing the particles to a target density of 1 gm/cm³. The internal bond strength and dimensional stability of the disks were evaluated based on Japanese standards. The experimental results showed that the internal bond strength and dimensional stability of the samples were enhanced as the particle size decreased. The microstructure of samples was investigated by field emission scanning electron microscopy (FE-SEM) coupled with energy dispersive X-ray analysis (EDXA). An X-ray diffraction (XRD) procedure was used to study the crystalline structure of binderless particleboard samples. The results indicated that different particle size did not change the crystalline structure, but the degree of crystallinity decreased when the particle size was decreased. The profile density distribution was estimated using an X-ray computed tomography (CT) scanner. The CT results indicated that samples having smaller particle size had lower variation of density distribution profile compared with those samples made with larger particle size. Based on the overall results of this study, raw material from *Rhizophora spp.* wood can be used to fabricate binderless particleboard without using any adhesives, and these could be used as a phantom in a radiotherapy center. This study indicated that particle size affected the sample properties.

Keywords: *Rhizophora spp.*; *Binderless particleboard*; FE-SEM; XRD; Density distribution; Computed Tomography (CT)

Contact information: a: School of Physics, Universiti Sains Malaysia, 11800 Penang, Malaysia; b: Div. of Bio-resource, Paper and Coatings Technology, School of Industrial Technology, Universiti Sains Malaysia, 11800 Penang, Malaysia; c: Physics Programme, School of Distance Education, Universiti Sains Malaysia, 11800 Penang, Malaysia; *Corresponding author: hrokiah@usm.my

INTRODUCTION

Mangroves tree and shrubs usually grow in saline (brackish) coastal habitats in the tropics and subtropics (Hogarth 1999). *Rhizophora spp.* is a type of mangrove wood that mainly can be used as fuel wood, charcoal, banda timber, and building material such as scaffolding and piling (Atheull et al. 2009).

There were some studies conducted that investigated the suitability of *Rhizophora spp.* as a tissue-equivalent material (Bradley and Tajuddin 1991; Che Wan Sudin 1993). Their studies showed that using mangrove wood, specifically *Rhizophora spp.*, yields results similar to water-equivalent materials. Further investigation of this wood (Tajuddin et al. 1996) showed that *Rhizophora spp.* and modified rubber have similar scattering and

radiographic properties to that of water. In addition, radiotherapy using high energy and electrons on this wooden phantom was carried out with other common standard phantoms (Banjade et al. 2001a,b). Generally, these experiments showed encouraging similarities in dosimetric properties between *Rhizophora spp.* and other standard phantom materials used in radiotherapy centers. However, we found that raw untreated *Rhizophora spp.* wood has some disadvantages if it were to be used as phantom material: the raw wood has the tendency to crack and warp with time, and there is difficulty in controlling the uniformity of properties throughout the plank or slab. Therefore, we propose that the *Rhizophora spp.* wood should be reduced into small particles and compressed into particleboard.

Particleboard is a wood-based panel product manufactured from varying particles of wood or other lignocellulosic materials and a binder, consolidated together under pressure and temperature (Anonymous 1996). Most of the resins currently used in the particleboard industry are formaldehyde-based adhesives, urea formaldehyde being the most commonly used adhesive in the industry (Harper 2002; Hashim et al. 2009). Available references based on using the formaldehyde adhesives to fabricate equivalent tissue phantom have not been found. A formaldehyde-based adhesive such as urea formaldehyde has a mass attenuation coefficient value of $0.18\text{cm}^2/\text{g}$ at energy of 60keV (Laufenberg 1986). We found that urea formaldehyde does not have the same attenuation property when used in tissue, having a mass attenuation coefficient of $0.208\text{cm}^2/\text{g}$ at same energy (Hubbell and Seltzer 1996). This dissimilarity makes urea formaldehyde unstable to be used in fabrication of a standard phantom. Additionally, urea formaldehyde emits formaldehyde from panels, which may cause health concerns (Hashim et al. 2011a,b). Therefore, manufacture of particleboards made without the use of any resins, known as the binderless particleboards, is an alternative way to ensure the regularity of distribution density of the final product from the same type of material. This implementation has a positive impact on the phantom used in medical radiation as well by keeping the final product free of any adverse health effects.

Strength of the self-bonding can be achieved through the activation of the chemical components of the board constituents during application of heat and pressure. Nevertheless, degradation of the hemicelluloses during heat and pressure treatment to produce simple sugars plays an important role in the strengthening mechanism due to self-bonding (Widyorini et al. 2005). Therefore, usually binderless particleboards are fabricated from non-woody raw materials, which are abundant in hemicelluloses (Mobarak et al. 1982; Ellis and Paszner 1994; Laemsak and Okuma 2000). This information has led to studies in particleboard manufactured without using synthetic adhesives from non-wood raw materials such as kenaf (Widyorini et al. 2005; Okuda et al. 2006), oil palm (Hashim et al. 2011b), and bark (Chow 1975). To date, information on binderless particleboard from *Rhizophora spp.* has been lacking, and no solid data has been reported on the properties of *Rhizophora spp.* binderless particleboard.

The properties of particleboards can be significantly affected by particle geometry, which includes the shape and particle size (Frybort et al. 2008). Another study (Suchsland and Woodson 1987) suggested that particle geometry plays a more significant role in the development of board properties than the actual mechanical properties of the fiber type panel. The variation of particle geometry has significant influence on the

strength properties of the particleboard (Biswas et al. 2010). In addition, Miyamoto et al. (2002) showed the effect of particle shape on the linear expansion of particleboard. The effect of particle size often was observed on internal bond strength of the boards (Ngueho Yemele et al. 2008). A study by Osarenmwinda and Nwachukwu (2007) showed that the smaller particle size gave better the properties of the particleboard. Hence, the internal bond strength of the boards mostly increased with decreasing bark particle size (Ngueho Yemele et al. 2008). On the other hand, it was shown that particle size strongly influences the density distribution of the panel (Steiner and Wei 1995; Kruse et al. 2000).

Regarding the density distribution measurement, Lazarescu et al. (2010) investigated X-ray computed tomography (CT) and found the method to be capable of measuring the interior properties of wood. Previous studies of CT scanning of wood showed that the CT system can be used to detect defects in logs and nondestructive measurements of wood density (Taylor et al. 1984; Lindgren 1991; Léonard et al. 2004; Alkan et al. 2007).

The objective of this study was to investigate the potentiality of a raw material from *Rhizophora spp.* wood, to be used to fabricate binderless particleboard without using any adhesive or heat. The internal bond strength (IB) and dimensional stability of samples were evaluated focusing on the effect of particle size. In addition, profile density distribution was investigated using X-ray Computed tomography (CT). The crystallinity characterization was carried out by X-ray diffraction spectrum. Field-emission scanning electron microscopy (FE-SEM) coupled with energy dispersive X-ray analysis (EDXA) were used to investigate the morphological properties and bonding quality of the different particle size of a raw material.

EXPERIMENTAL

Materials

The *Rhizophora spp.* trunks were obtained directly from one of the mangrove reserve forests in Kuala Sepetang, Perak, Malaysia with the help of experienced forestry officers. The trunks were from middle stem of *Rhizophora spp.* with $1 \pm 0.1\text{m}$ length. Based on the study by Shakhreer et al. (2009) the middle part of *Rhizophora spp.* has a mass attenuation coefficient value that is very close to the calculated value for young-age breast (Breast 1) (Constantinou 1982). The trunks were sawn horizontally into four boards with thicknesses approximately equal. The boards were passed through the surface planner machine model (Holy Tek- HP 20, Taiwan). This was repeated many times until the board had been reduced to a very thin layer, and chips resulting from this process were gathered. The *Rhizophora spp.* chips were then reduced into small particles using the hammer-milling. A laboratory oven was used to dry the small particles to 7-8% moisture content. All particles were ground many times using a Willey Mill model (Retsch, Germany) to get fine particles from *Rhizophora spp.* wood. To classify the particle size, a horizontal screening machine was used with three sieves opening of 147, 74, and $50\text{ }\mu\text{m}$ to remove oversize and undersize of the *Rhizophora spp.* particles. A sample of the different sizes of the particles can be seen in Fig. 1.



Fig. 1. *Rhizophora spp.* particles (from left to right fractions retained on the following sieves: 147 - 74, 74 - 50 and <50 μm)

Methods

Samples preparation

A total of 75 sample disks with a diameter of 25 mm were made. Twenty-five disks were made from each particle size for the experiments. All disks were manually formed using a stainless steel mould, as shown in Fig. 2. The *Rhizophora spp.* particles were compressed into disks for 20 seconds at 34.5 MPa by using a manual hydraulic press machine. For each particle size, disks with target density and thickness of $1.00 \pm 0.1 \text{ g/cm}^3$ and $0.5 \pm 0.01 \text{ cm}$, respectively, were produced. Table 1 classifies *Rhizophora spp.* disk samples based on particle size, and the measured densities that were used in this study.



Fig. 2. Stainless steel mould

Table 1. *Rhizophora spp.* Disk Samples with Different Particle Size and Measured Density

Sample	Particle size (μm)	Measured density (g/cm^3)			
		Average	Max	Min	Standard deviation
A	147 - 74	1.047	1.057	1.036	0.005
B	74 - 50	1.071	1.098	1.065	0.006
C	<50	1.115	1.125	1.105	0.005

Test procedure

Internal bond strength (IB) was carried out based on standard method Japanese Industrial Standard (JIS, A-5908) with modification of size of test specimens. Eight IB samples of size 490.87 mm² were prepared from each type of particle size. The IB test was carried out on an Instron Testing System Model UTM-5582 (USA) equipped with a load cell having a capacity of 1000 kg. Six samples were used to study the dimensional stability of the samples in terms of water absorption (WA) for a few second of water soaking.

Microstructure study

Field emission scanning electron microscopy (FE-SEM) investigations were carried out to determine the morphological properties of the raw materials and their parenchyma cells in the samples related to bonding quality between the different particle sizes of material. Micrographs were taken from cross sections of 0.5 cm by 0.5 cm of binderless disks from the different particle sizes of *Rhizophora spp.* wood. The samples were carefully mounted on specimen holders and coated with gold by an ion sputter coater (Polaron SC515, Fisons Instruments, UK). A Field Emission Scanning Electron Microscope LEO Supra 50 Vp, Carl-Zeiss SMT, Oberkochen, Germany was used for microscopic study. In addition, the elemental composition of the *Rhizophora spp.* particles was obtained by energy dispersive X-ray analysis (SEM-EDXA).

Characterization of the crystallinity

X-ray diffraction (XRD) with a wide angle was carried out to investigate the crystallographic structure and orientation of the different types of *Rhizophora spp.* particles. A high resolution (Hr) X-ray diffractometer (PANalytical X'Pert Pro MRD) from Rigaku diffractometer was used with a Cu-K_{α1} radiation source ($\lambda = 1.5406 \text{ \AA}$) generated at an operating voltage and a current of 40kV and 30mA, respectively. The Cu K_{α1} radiation was filtered electronically with a thin Ni-filter. A 2θ angle range from 10° to 40° in reflection mode was scanned at 2°/min. The Crystallinity Index was calculated according to the previous study (Segal et al. 1959), to quantify the crystallinity of the samples. The Crystallinity Index (CI_n) is defined by,

$$CI_n = 100 \times (I_{\text{crystalline}} - I_{\text{amorphous}}) / I_{\text{crystalline}} \quad (1)$$

where $I_{\text{crystalline}}$ is the peak intensity corresponding to crystalline, and $I_{\text{amorphous}}$ is the peak intensity of the amorphous fraction.

X-ray computed tomography scanning

The X-ray CT scanner (Somaton Sensation Open, Siemens, Germany) used in this study was developed recently by Siemens to test the inside of materials. The machine settings were 120 kVp and 33 mA. Tungsten is used as the target for X-ray. The sample is rotated incrementally within the X-ray beam to measure the transmission of the X-ray. The CT number is represented as Hounsfield (HU) units, which is related to the density. HU = 0 means standard for the density of water (1.0 g/cm³) and HU= -1000 for air. When HU values are positive, they represent a material with density above (1.0 g/cm³). A linear

relation between *CT*-numbers and wood density was developed (Lindgren 1991). This relation could not be applied directly in other experiments because there are significant differences in the *CT* numbers between scanners from different manufacturers, and even among scanners from the same manufacturer and model (Levi et al. 1982). Therefore, it was established that a calibration curve needs to be obtained by scanning the uniform reference test sample with known the moisture content, density, and oven-dried density (Levi et al. 1982). From the calibration curve, the relation between the *CT* number and density can be obtained accurately (Lindgren 1991). In this experiment, adjusting the X-ray CT scanner was unsuitable to obtain the absolute value for density, and we need to show the distribution of profile density in the binderless particleboard of the *Rhizophora spp.* disks. Accordingly, we used *CT* numbers of (-1000) and (0) for air and water respectively, as a standard calibration curve. For demonstrating this linear correlation, an aluminum metal plate (99.99% purity) was scanned and used as a standard material as shown in Fig. 3.

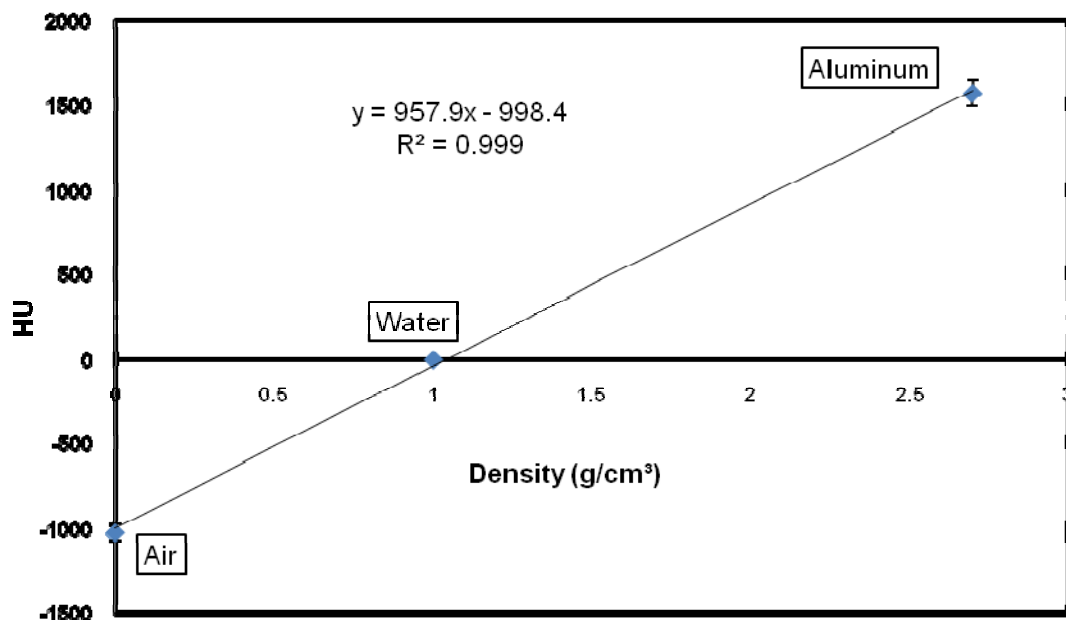


Fig. 3. Calibration curve between Hounsfield (HU) unit and standard samples density

The density (ρ) measured according to the calibration curve could be obtained by:

$$\rho = (CT + 998.48)/957.96 \quad (2)$$

The true physical density of each disk was calculated simply by dividing the mass (g) to measured volume (cm^3). Each disk was scanned using about 38 rays, each 0.6 mm thick with a 0.6 mm incremental table movement. The area of interest was studied as a circular area of 0.03 cm^2 . For each slice scan, a four circular area of interest was indicated to occupy about 80% of the cross-sectional area of the rectangular square cross-section in order to minimize pixel averaging at the edges. The *CT* number for each

interested area was recorded, and the values for the two end scans were neglected, once more to reduce the pixel averaging effect at the wood-air interface. The 34 or 35 other *CT* number values were determined. The average *CT* numbers for all interested areas were computed. Consequently, the densities of each slice level of binderless particleboard disks were estimated by using Eq. 2. Afterwards, the density distribution profile was investigated.

RESULTS AND DISCUSSION

Internal Bond Strength and Water Absorption Property

The average internal bond strength (*IB*) values of the specimens manufactured from several particle sizes are illustrated in Fig. 4. The *IB* values of binderless particleboard made from *Rhizophora spp.* wood were 0.015, 0.020, and 0.080 N/mm² for samples A, B, and C, respectively, which are below the values specified by the Japanese Industrial Standard A 5908. The Japanese Industrial Standard, JIS A-5908, Type-8 minimum requirement for *IB* is 0.15 N/mm². However, this was expected, since no adhesive, and heat was used during disk making. From this, it can be seen that *IB* values obviously decreased with increasing the particle size of samples. The *IB* values of sample C were 81.25 % and 75 % higher than those from samples A and B, respectively. The smaller particle size results in particles being more compressed, seen mostly as attached vessel elements and parenchymatous cells, causing better strength characteristics of the samples. Effect of particle size on *IB* property was also investigated in various previous studies, and it was found that the *IB* value of the disks frequently decreased with increasing the particle size of disk, as can be seen in aspen bark (Ngueho Yemele et al. 2008) and rice husk (Osarenmwinda and Nwachukwu 2007).

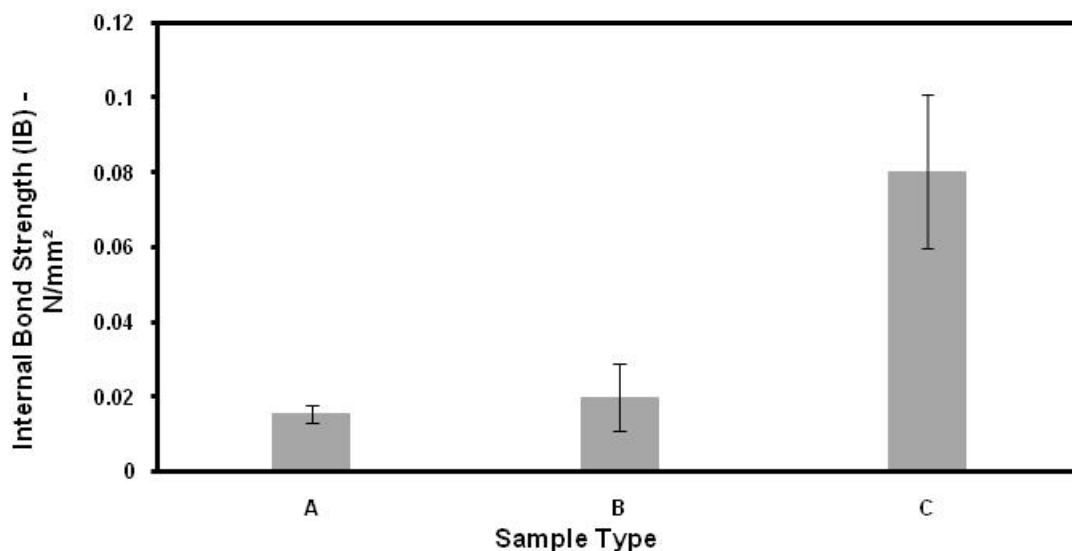


Fig. 4. Average internal bond strength values of the *Rhizophora spp.* binderless particleboard samples A, B and C, each sample has different particle size of 147-74(μm), 74 – 50 (μm) and <50 (μm) respectively

The three types of binderless particleboard from *Rhizophora spp.* showed a high effect of water absorption. The samples did not remain stable for a long time, and they disintegrated relatively quickly. Therefore, we studied the difference of the time period for the sample to start to disintegrate in water during soaking. Fig. 5 showed slightly different results in the samples. Sample C had a slightly longer time of stability of 6.99 s/density, which was 26.7 % and 7.32 % higher than samples A and B, respectively. In fact, the main purpose of binderless particleboard of *Rhizophora spp.* is to fabricate a phantom that could be used in medical physics centers. Consequently, it will be used without touching water, which reduces the risk of water effect on the phantom. It was suggested to add some processes such as steam treatment and heat treatment. These methods could be considered to improve the dimensional stability and reduce the tendency to absorb water (Mobarak et al. 1982; Widyorini et al. 2005).

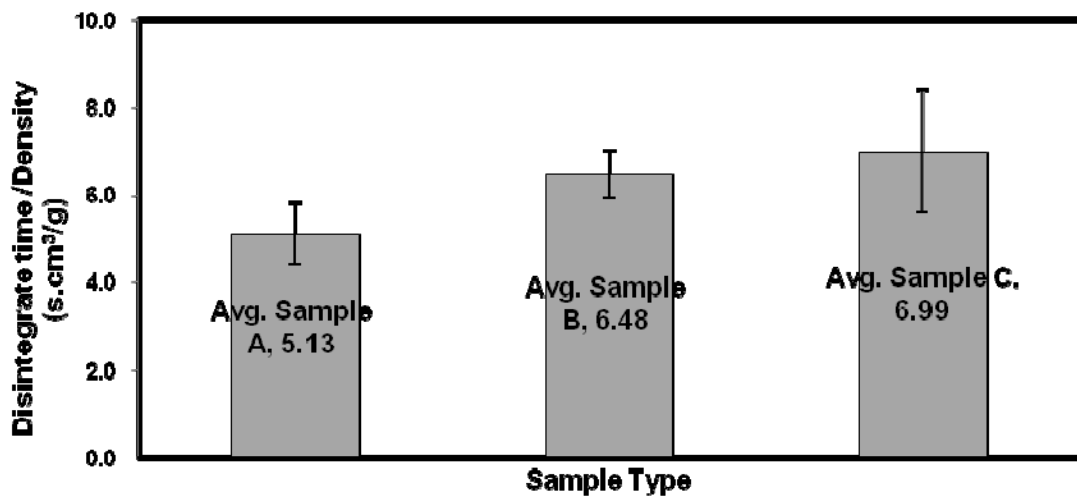


Fig. 5. Average fractions disintegrate time to the density values of the samples A, B and C

Microstructure Analysis

Micrographs were used to study binderless particleboards as a function of particle size. The FESEM micrographs of the samples made from three types of particle size: (147-74 μm), (74-50 μm), and (<50 μm) are shown in Figs. 6, 7, and 8, respectively. Disk made from larger particles had more void spaces (see arrow). Smaller particle size, as in Figs. 7 and 8, showed a reduction in void space. The reduced void space will produce a smoother surface compared to those having bigger particle size, as showed in Fig. 6. All samples showed compression of cell lumens. The compressed fiber walls during pressing are depicted in Figs. 6, 7 and 8. This will result in the reduction of lumen void space and thus increased the density of the disk produced. The variation of particle size results in different specific surface areas, which have significant impacts on the board properties (Moslemi 1974). Generally, the specific surface area of the particle size increased with decreasing the particle size. The FESEM of the samples made from smaller particle size (sample C) (Fig. 8) manifested a uniform homogenous merge of the cells which were compressed together. This led to a smoother surface of the sample made from smaller particle size (sample C) (Fig. 8) as compared to Fig. 6 and 7.

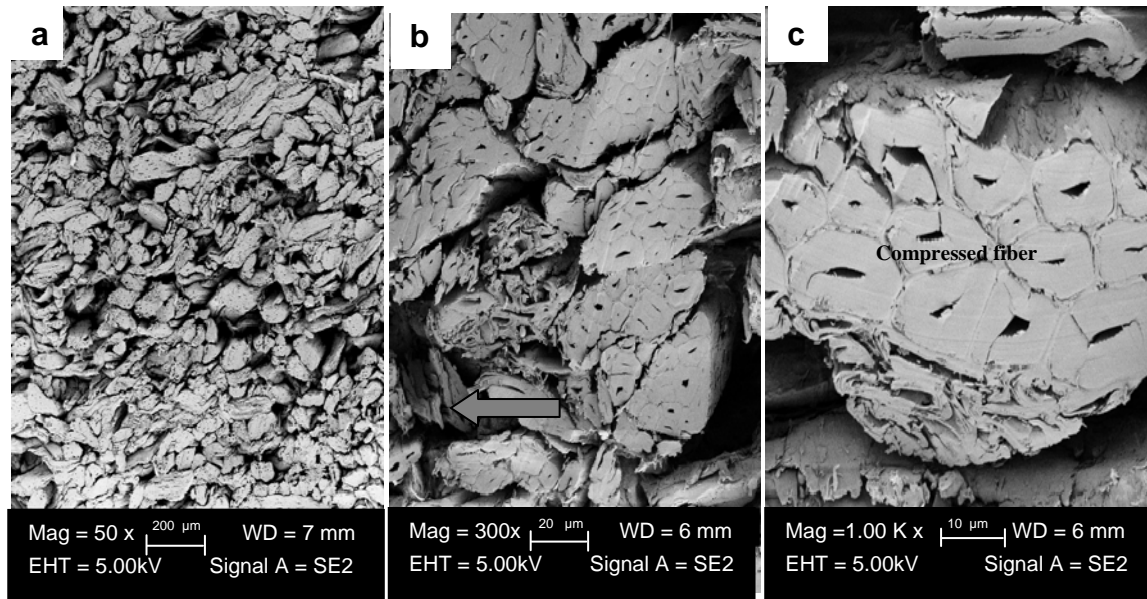


Fig. 6. Micrographs of cross section of binderless particleboard made from sample A with (147-74 μm) particle size of *Rhizophora* spp. wood at different magnification

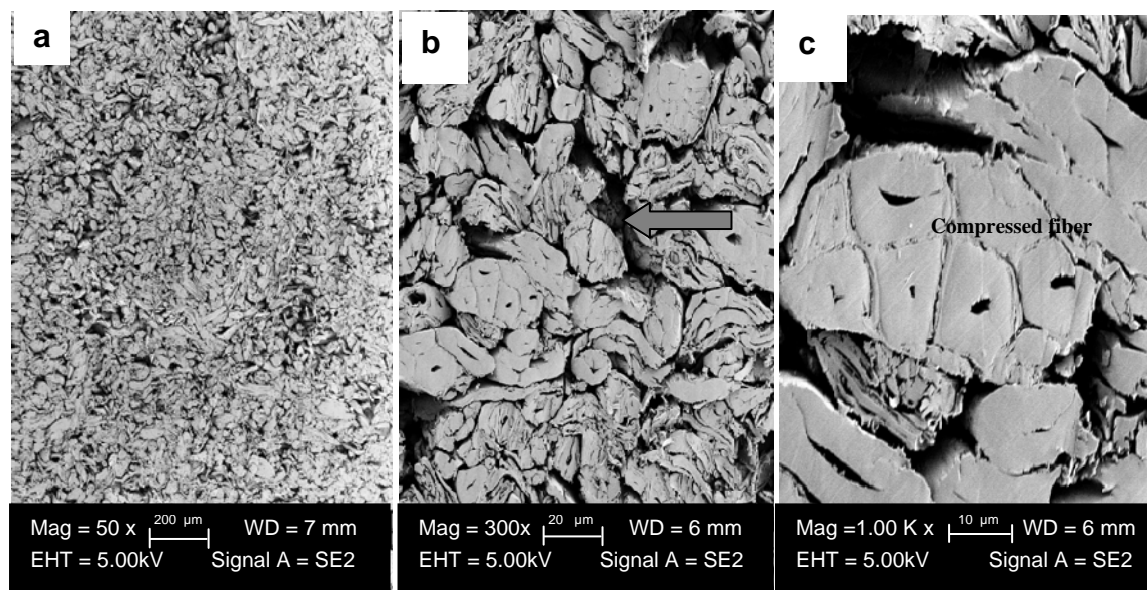


Fig. 7. Micrographs of cross section of binderless particleboard made from sample B with (74-50 μm) particle size of *Rhizophora* spp. wood at different magnification

It appears that smaller particle size (sample C) contributed to a higher internal bond strength (IB) value as compared to samples A and B. Smaller particle size results increased the ratio of lumen to the vessel wall, which increased the ability of the particles to be compressed together (Fig. 8).

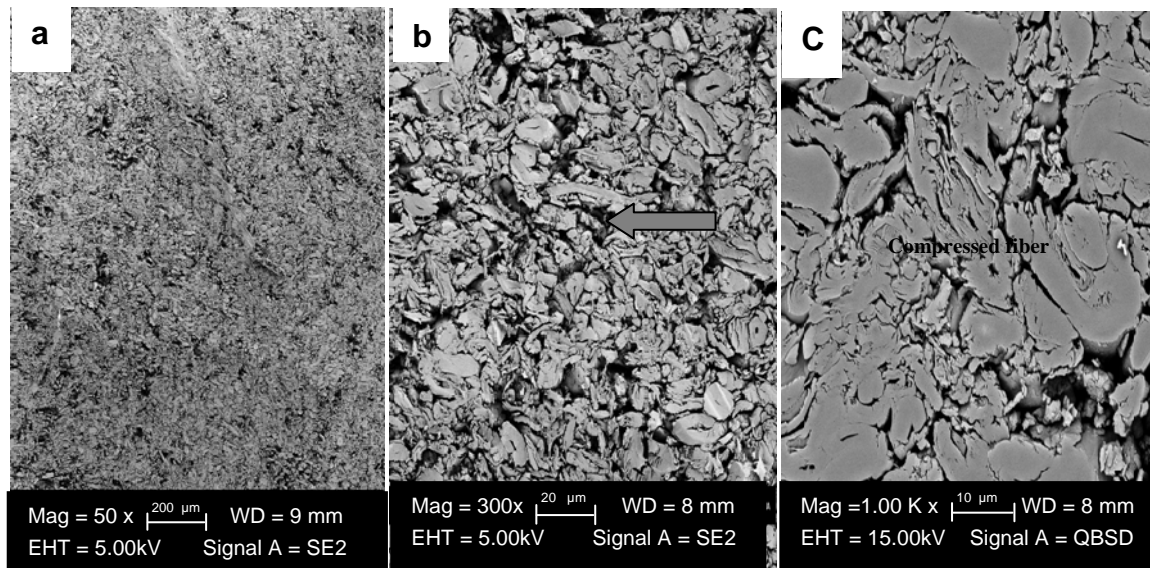


Fig. 8. Micrographs of cross section of binderless particleboard made from sample C with (<50 μm) particle size of *Rhizophora spp.* wood at different magnification

Scanning electron microscopy equipped with energy dispersive X-ray analysis (SEM-EDXA) was used to study inorganic constituents of the particleboards made from three particle sizes of *Rhizophora spp.* wood. Figure 9 shows the EDXA spectrum measured from the sample C to illustrate the spectrum and elemental composition. Based on EDXA spectrum results of binderless particleboards samples A, B, and C, no there were significant differences. All specimens had high weight percentage of carbon and oxygen, while little nitrogen was determined (Che Wan Sudin 1993). According to EDXS spectrum measurements, the binderless particleboard of *Rhizophora spp.* showed no specific change in the percentage of elemental composition. This indicates potential for use of binderless particleboard of *Rhizophora spp.* as a phantom in radiotherapy centers.

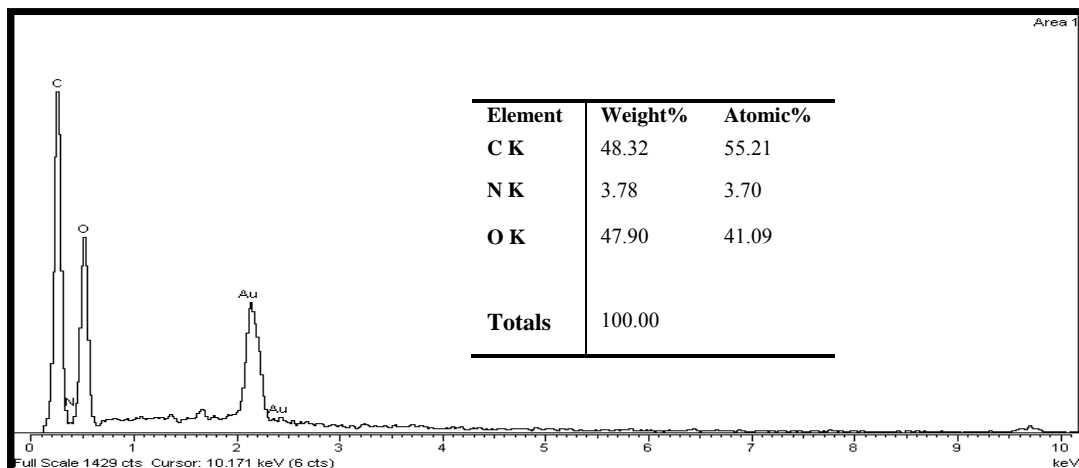


Fig. 9. EDXA spectrum and elemental composition of binderless particleboard of *Rhizophora spp.* made from sample C

X-ray Diffraction Analysis

X-ray diffraction (XRD) is a non-destructive technique that is widely used in material characterization, particularly to determine crystallographic structure and orientation, crystalline quality and residual strain of the crystalline structure as well as chemical composition of natural and manufactured materials (Li et al. 2009). There are some studies on applying the XRD to study the relative crystallinity in the wood (Lotfy et al. 1974; Tanaka et al. 1981; Dwianto et al. 1996; Kubojima et al. 1997).

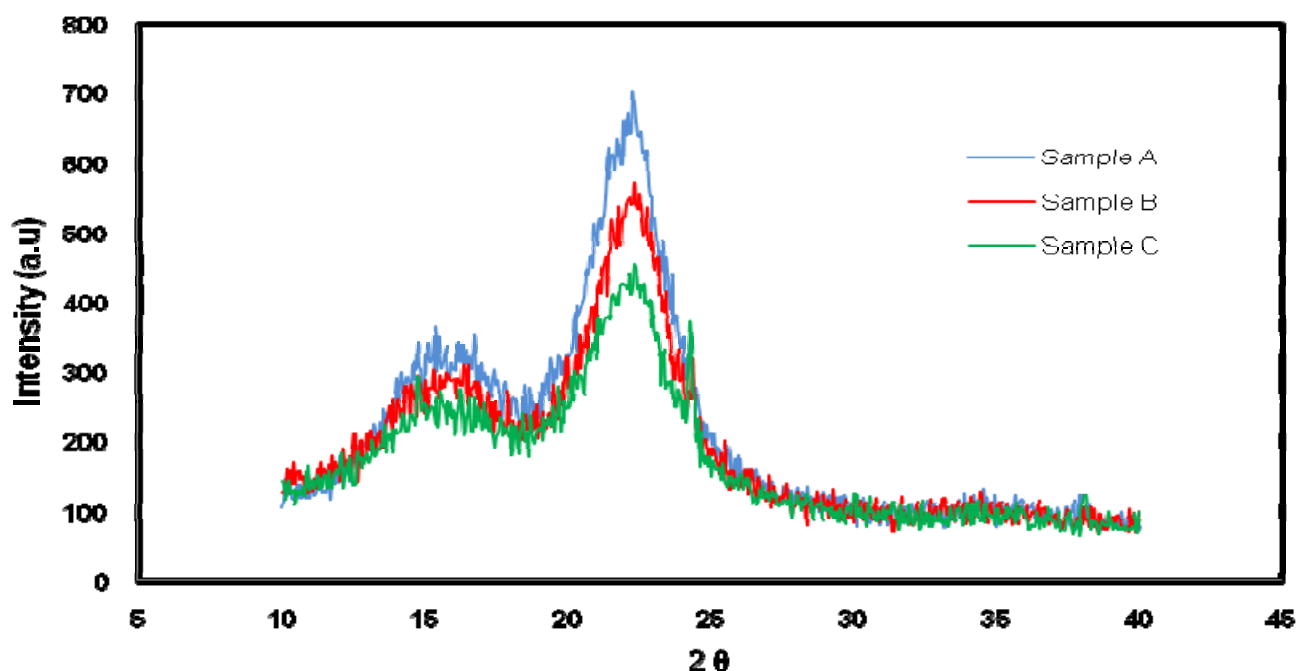


Fig. 10. XRD diffraction patterns of the binderless particleboard samples (sample A, B, and C)

Typical results of the X-ray diffraction spectra of the cellulose samples are shown in Fig. 10. The calculated values of crystallinity index of the binderless particleboard samples are listed in Table 2. As shown in Fig. 10, the XRD diffraction pattern of samples A, B, and C showed a major peak intensity at the diffraction angle $2\theta = 22.8^\circ$ and two secondary peaks at $2\theta = 14^\circ$ and $2\theta = 16^\circ$. Sample C showed a clear decrease in the intensity of major peak and also the secondary peaks at $2\theta = 14^\circ$ and $2\theta = 16^\circ$. There were no crystalline transformations in the structures of the samples, but there were different crystallinity levels. The crystallinity indices of the samples A, B, and C were calculated according to Segal et al. (1959) and were found to be equal to 67.5, 64.5, and 60.8 %, respectively as shown in Table 2. The degree of crystallinity of cellulose was found to be higher in the sample A than in the samples B and C. These changes in the crystallographic pattern of cellulose were observed due to damage of the crystalline structures of cellulose samples during milling and hence decreased the crystallinity. However, XRD diffraction analysis indicated that the crystallinity of binderless particleboard decreased as the particle size decreased.

Table 2. Crystallinity of Binderless Particleboard Samples of *Rhizophora spp.*

Sample	A	B	C
Crystallinity, %	67.5	64.5	60.8

Density Distribution Profile

The calculated density of the binderless particleboard samples (A, B and C) and mean, maximum, minimum, and standard deviation of the CT numbers are presented in Table 3. It can be seen that the CT number increases with decreasing particle size of *Rhizophora spp.* samples; the smaller particle size (sample C) had a larger CT number with a standard deviation 24.96, compared with samples A and B, with a standard deviation 37.69 and 25.60, respectively. By the relationship between CT number and wood density, this effect can be attributed to particle size of the binderless particleboard.

Table 3. Measured Density and Mean, Maximum, Minimum, and Standard Deviation of the CT Number

Sample	CT Number				Calculated density (g/cm ³)
	Mean	Maximum	Minimum	Standard deviation	
A	96.24	131.40	-46.10	37.69	1.051
B	154.62	192.30	59.80	25.60	1.082
C	233.11	270.80	168.80	24.96	1.124

The relative density distribution profiles across the width of the binderless particleboards are presented in Fig. 11. From the density profile measured using equation (2), it was found that all of the samples had disparately uniform horizontal density distribution along the disk samples irrespective of the sample mean density levels. To clarify the profile density variation across the binderless particleboard samples, the CT number values for the two or three beginning and end scans were not considered in order to reduce the effect of decadence of the density at the edge of samples. Therefore, the interest region along the disk samples was 1.2 to 21.6 mm, as shown in Fig. 11. Typically, the variability of the density distribution of a disk samples was described by its coefficient of variation (COV), where COV is the ratio of the density standard deviation to its average density.

Table 4 summarizes the calculated COV's along with the maximum and minimum density values for the binderless particleboard samples. According to COV values, it is evident that sample C was considerably uniform in the density compared to samples A and B, where the smaller particle size of disk samples (B and C) showed slight ratios of the COV values of 2.220 % and 2.027 % respectively. In addition, the larger particle size sample A had COV 3.443 %, which led to a less uniform density distribution. In general, it can be stated that lower density variations were found from binderless particleboards made with smaller particles than for binderless particleboards made with larger particles. This is because when particle size increased, the number of voids between particles decreased in a limit area within one layer, while the size of voids

increased. Therefore, smaller particles lead to smaller overlapping areas, thinner voids between particles, and more chance for random distribution.

Binderless *Rhizophora spp.* Particleboards that are produced with different particle sizes results in variation of density distribution. By taking this into consideration, *Rhizophora spp.* binderless particleboard could be used as a phantom material in radiotherapy centers. Therefore, it is especially important to control the distribution of mass weight per area during binderless particleboard mat forming via control of the processing and improvement the equipment.

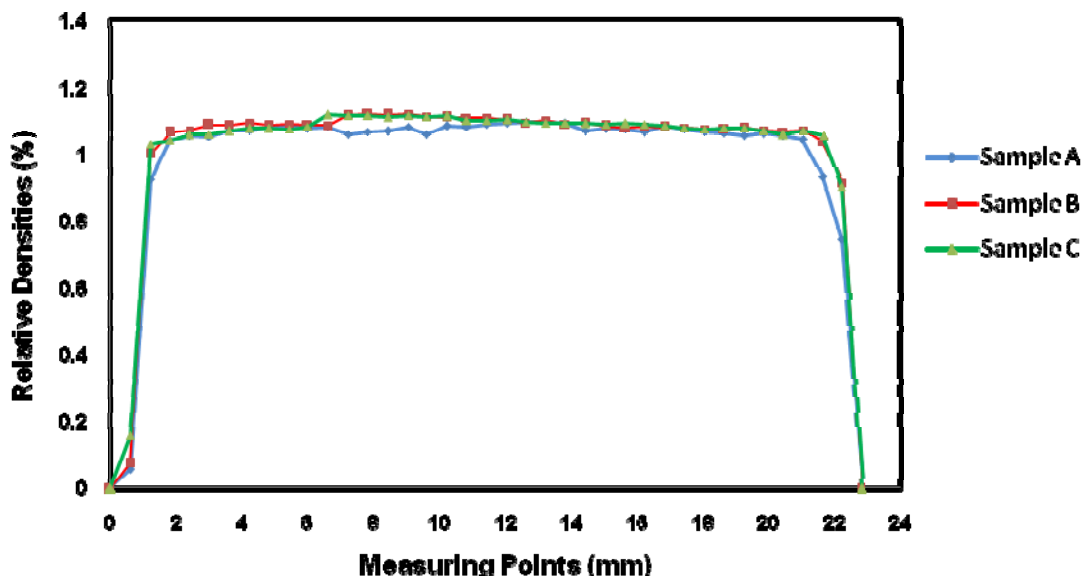


Fig. 11. Relative density profiles along the disk of the binderless particleboards samples A, B and C. All densities were normalized at their mean densities

Table 4. Results of Statistical Analyses Showing the Calculated Coefficient of Variation (COV), Maximum and Minimum Density Values of the Binderless Particleboard Samples by using CT Scan for Interest Region along the Disk Samples of 1.2 to 21.6 mm

Sample	COV %	Max (g/cm ³)	Min (g/cm ³)
A	3.443	1.179	0.994
B	2.220	1.243	1.105
C	2.027	1.325	1.219

CONCLUSIONS

1. In conclusion, the results of this study indicated the possibility of making binderless particleboard from raw material of *Rhizophora spp.* wood, to be used as a phantom in radiotherapy centers.

2. Particle size was found to have an effect on the Internal Bond (*IB*) strength and dimensional stability properties of the binderless particleboard fabricated from particles of three different sizes. However, these properties could be improved by using hot pressing temperature in the preparation of the disk samples.
3. Microscopic study using FE-SEM showed the correlation of compressed cell lumen, which revealed that samples made from smaller particle size, had better bonding strength characteristics and higher specific surface area.
4. X-ray diffraction analysis indicated a decrease, relatively, in the crystallinity index of samples made from smaller particle size.
5. X-ray computed tomography (CT) scanner showed that particle size influences the profile density distribution of samples, whereas binderless particleboard made from smaller particle size results in smaller variation of density distribution.

ACKNOWLEDGMENTS

We would like to acknowledge the financial support of Research University Grant 1001/PJJAUH/813007 from Universiti Sains Malaysia. We are grateful to Medical Image Unit of Mt Miriam Cancer Center in Penang, Malaysia for their kind permission to use the computed tomography (CT) scanner. The Forest Department of Kuala Sepetang Perak is also acknowledged for the Rhizophora wood samples.

REFERENCES CITED

- Alkan, S., Zhang, Y., and Lam, F. (2007). "Moisture distribution changes and wetwood behavior in subalpine fir wood during drying using high X-ray energy industrial CT scanner," *Drying technology* 25(3), 483-488.
- Anonymous (1996). "Particleboard - from start to finish," National Particleboard Association. Gaithersburg, Maryland, USA.
- Atheull, A. N., Din, N., Longonje, S. N., Koedam, N., and Dahdouh-Guebas, F. (2009). "Commercial activities and subsistence utilization of mangrove forests around the Wouri estuary and the Douala-Edea reserve (Cameroon)," *Journal of Ethnobiology and Ethnomedicine* 5(1), 35.
- Banjade, D. B., Tajuddin, A. A., and Shukri, A. (2001a). "Determination of absorbed dose for photon and electron beams from a linear accelerator by comparing various protocols on different phantoms," *Applied Radiation and Isotopes* 55(2), 235-243.
- Banjade, D. B., Tajuddin, A. A., and Shukri, A. (2001b). "A study of *Rhizophora spp* wood phantom for dosimetric purposes using high-energy photon and electron beams," *Applied Radiation and Isotopes* 55(3), 297-302.
- Biswas, D., Kanti Bose, S., and Mozaffar Hossain, M. (2010). "Physical and mechanical properties of urea formaldehyde-bonded particleboard made from bamboo waste," *International Journal of Adhesion and Adhesives* 31(2), 84-87.

- Bradley, D., and Tajuddin, A. A. (1991). "Photon attenuation studies on tropical hardwoods," *International Journal of Radiation Applications and Instrumentation. Part A. Applied Radiation and Isotopes* 42(8), 771-773.
- Che Wan Sudin, C. W. A. (1993). "Kayu tropika sebagai bahan tara setaraan tisu untuk kajian dosimetri," M.Sc. Thesis, Universiti Sains Malaysia.
- Chow, S. (1975). "Bark boards without synthetic resins," *Forest Products Journal* 25(11), 32-37.
- Constantinou, C. (1982). "Phantom materials for radiation dosimetry. I. Liquids and gels." *British Journal of Radiology* 55(651), 217.
- Dwianto, W., Tanaka, F., Inoue, M., and Norimoto, M. (1996). "Crystallinity changes of wood by heat or steam treatment," *Wood Research: Bulletin of the Wood Research Institute Kyoto University* 83, 47-49.
- Ellis, S., and Paszner, L. (1994). "Activated self-bonding of wood and agricultural residues," *Holzforschung-International Journal of the Biology, Chemistry, Physics and Technology of Wood* 48(s1), 82-90.
- Frybort, S., Mauritz, R., Teischinger, A., and Müller, U. (2008). "Cement bonded composites – A mechanical review," *BioResources* 3(2), 602-626.
- Harper, C. A. (2002). *Handbook of Plastics, Elastomers, and Composites*, McGraw-Hill Professional.
- Hashim, R., Hamid, S. H. A., Sulaiman, O., Ismail, N. Ibrahim, M. H., Jais, H., and Ujang, S. (2009). "Extractable formaldehyde from waste medium density fibreboard," *Journal of Tropical Forest Science* 21(1), 25-33.
- Hashim, R., Sarmin, S. N., Sulaiman, O., and Yusof, L. H. M. (2010). "Effects of cold setting adhesives on properties of laminated veneer lumber from oil palm trunks in comparison with rubberwood," *European Journal of Wood and Wood Products* 1-9.
- Hashim, R., Nadhari, W. N. A. W., Sulaiman, O., Kawamura, F., Hiziroglu, S., Sato, M., Sugimoto, T., Seng, T. G., and Tanaka, R. (2011). "Characterization of raw materials and manufactured binderless particleboard from oil palm biomass," *Materials & Design* 32(1), 246-254.
- Hogarth, P. J. (1999). *The Biology of Mangroves*, Oxford University Press (OUP).
- Hubbell, J. H., and Seltzer, S. M. (1996). "Tables of x-ray mass attenuation coefficients and mass energy-absorption coefficients," *National Institute of Standards and Technology*.
- Japanese Industrial Standard (JIS). (2003). JIS - A 5908. "Particleboard," Japanese Standard Association. 1-24, Akasaka 4, Minato-ku . Tokyo, Japan.
- Kruse, K., Dai, C., and Pielasch, A. (2000). "An analysis of strand and horizontal density distributions in oriented strand board (OSB)," *European Journal of Wood and Wood Products* 58(4), 270-277.
- Kubojima, Y., Okano, T., and Ohta, M. (1997). "Effect of annual ring widths on structural and vibrational properties of wood," *Journal of the Japan Wood Research Society (Japan)* 43(8), 634-641.
- Laemsak, N., and Okuma, M. (2000). "Development of boards made from oil palm frond II: properties of binderless boards from steam-exploded fibers of oil palm frond," *Journal of Wood Science* 46(4), 322-326.

- Laufenberg, T. L. (1986). "Using gamma radiation to measure density gradients in reconstituted wood products," *Forest Prod. J* 36(2), 59-62.
- Lazarescu, C., Watanabe, K., and Avramidis, S. (2010). "Density and moisture profile evolution during timber drying by CT scanning measurements," *Drying Technology* 28(4-6), 460-467.
- Léonard, A., Blacher, S., Marchot, P., Pirard, J. P., and Crine, M. (2004). "Measurement of shrinkage and cracks associated to convective drying of soft materials by X-ray microtomography," *Drying technology* 22(7), 1695-1708.
- Levi, C., Gray, J. E., McCullough, E., and Hattery, R. (1982). "The unreliability of CT numbers as absolute values," *American Journal of Roentgenology* 139(3), 443.
- Li, Y., Wong, C., and Lu, D. (2009). *Electrical Conductive Adhesives with anotechnologies*, Springer Verlag, 104-105.
- Lindgren, L. (1991). "Medical CAT-scanning: X-ray absorption coefficients, CT-numbers and their relation to wood density," *Wood Science and Technology* 25(5), 341-349.
- Lotfy, M., El-Osta, M., Kellogg, R., Foschi, R., and Butters, R. (1974). "A mechanistic approach to crystallite length as related to cell-wall structure," *Wood and Fiber Science* 6(1), 36-45.
- Miyamoto, K., Nakahara, S., and Suzuki, S. (2002). "Effect of particle shape on linear expansion of particleboard," *Journal of Wood Science* 48(3), 185-190.
- Mobarak, F., Fahmy, Y., and Augustin, H. (1982). "Binderless lignocellulose composite from bagasse and mechanism of self-bonding," *Holzforschung-International Journal of the Biology, Chemistry, Physics and Technology of Wood* 36(3), 131-136.
- Moslemi, A. (1974). *Particleboard. Volume 1: materials*, Southern Illinois University Press, Carbondale, Illinois.
- Ngueho Yemele, M. C., Blanchet, P., Cloutier, A., and Koubaa, A. (2008). "Effects of bark content and particle geometry on the physical and mechanical properties of particleboard made from black spruce and trembling aspen bark," *Forest Products Journal* 58(11), 48-56.
- Okuda, N., Hori, K., and Sato, M. (2006). "Chemical changes of kenaf core binderless boards during hot pressing (II): effects on the binderless board properties," *Journal of Wood Science* 52(3), 249-254.
- Osarenmwinda, J., and Nwachukwu, J. (2007). "Effect of particle size on some properties of Rice Husk Particleboard," *Advanced Materials Research* 18, 43-48.
- Segal, L., Creely, J., Martin, A., and Conrad, C. (1959). "An empirical method for estimating the degree of crystallinity of native cellulose using the X-ray diffractometer," *Textile Research Journal* 29(10), 786.
- Shakhreet, B., Bauk, S., Tajuddin, A., and Shukri, A. (2009). "Mass attenuation coefficients of natural *Rhizophora spp.* wood for X-rays in the 15.77–25.27 keV range," *Radiation Protection Dosimetry*, 135(1), 47.
- Steiner, P. R., and Wei, X. (1995). "Influence of flake characteristics on horizontal density distribution of flakeboard," *Forest Products Journal* 45(4), 61-66.
- Suchsland, O., and Woodson, G. E. (1987). *Fiberboard Manufacturing Practices in the United States*, US Dept. of Agriculture, Forest Service.

- Tajuddin, A. A., Che Wan Sudin, C., and Bradley, D. (1996). "Radiographic and scattering investigation on the suitability of *Rhizophora sp.* as tissue-equivalent medium for dosimetric study," *Radiation Physics and Chemistry* 47(5), 739-740.
- Tanaka, F., Koshijima, T., and Okamura, K. (1981). "Characterization of cellulose in compression and opposite woods of a *Pinus densiflora* tree grown under the influence of strong wind," *Wood Science and Technology* 15(4), 265-273.
- Taylor, F. W., Wagner Jr, F. G., McMillin, C. W., Morgan, I. L., and Hopkins, F. F. (1984). "Locating knots by industrial tomography. A feasibility study," *Forest Products Journal* 34(5), 42-46.
- Widyorini, R., Xu, J., Watanabe, T., and Kawai, S. (2005). "Chemical changes in steam-pressed kenaf core binderless particleboard," *Journal of Wood Science* 51(1), 26-32.

Article submitted: April 27, 2011; Peer review completed: July 23, 2011; Revised version received and accepted: August 20, 2011; Published: August 22, 2011.